

# Measurement of the forward backward asymmetry of $c$ and $b$ quarks at the $Z$ pole using reconstructed $D$ mesons

Preliminary

DELPHI Collaboration

Th. Brenke<sup>1</sup>, M. Elsing<sup>2</sup>, P.Sponholz<sup>1</sup>

## Abstract

A measurement of the forward-backward asymmetry of  $e^+e^- \rightarrow c\bar{c}$  and  $e^+e^- \rightarrow b\bar{b}$  on the  $Z$  resonance is performed using about 3 million hadronic  $Z$  decays collected by the DELPHI detector at LEP in the years 1992 to 1995. The heavy quark is tagged by the exclusive reconstruction of  $D$  meson decays in the modes  $D^{*+} \rightarrow D^0\pi^+$ ,  $D^0 \rightarrow K^-\pi^+$  and  $D^+ \rightarrow K^-\pi^+\pi^+$ . The forward-backward asymmetries for  $c$  and  $b$  quarks at the  $Z$  resonance are determined to be:

$$A_{\text{FB}}^c = 0.0658 \pm 0.0093 (\text{stat}) \pm 0.0042 (\text{syst})$$

$$A_{\text{FB}}^b = 0.0766 \pm 0.0190 (\text{stat}) \pm 0.0099 (\text{syst})$$

Paper submitted to the ICHEP'98 Conference  
Vancouver, July 22-29

<sup>1</sup> Bergische Universität – Gesamthochschule Wuppertal, Germany

<sup>2</sup> CERN, Geneva, Switzerland

# 1 Introduction

The precise measurement of the forward-backward asymmetry of the process  $e^+e^- \rightarrow Z \rightarrow f\bar{f}$  is a fundamental test of the standard model and allows to determine the weak mixing angle  $\sin^2\theta_{eff}^{lep}$ . In this analysis, the forward-backward asymmetries for the processes  $e^+e^- \rightarrow c\bar{c}$  and  $e^+e^- \rightarrow b\bar{b}$  at the  $Z$  resonance are measured using reconstructed  $D$  mesons in the modes <sup>1</sup>:

$$\begin{aligned}
 D^{*+} &\rightarrow D^0\pi^+ \\
 &\rightarrow (K^-\pi^+)\pi^+ \\
 &\rightarrow (K^-\pi^+\pi^-\pi^+)\pi^+ \\
 &\rightarrow (K^-\pi^+(\pi^0))\pi^+ && \text{with and without } \pi^0 \text{ reconstruction} \\
 &\rightarrow (K^-\mu^+(\nu_\mu))\pi^+ \\
 &\rightarrow (K^-e^+(\nu_e))\pi^+ \\
 D^0 &\rightarrow K^-\pi^+ \\
 D^0 &\rightarrow K^-\pi^+(\pi^0) && \text{no } \pi^0 \text{ reconstruction} \\
 D^+ &\rightarrow K^-\pi^+\pi^+
 \end{aligned}$$

The information of the particle identification from the ring imaging Cherenkov counter, the specific energy loss ( $dE/dx$ ) in the TPC, electron and muon identification and  $\pi^0$  reconstruction is used to identify the  $D$  decay products and to reduce combinatorial background.

It is necessary to distinguish between the contributions of  $D$  mesons from  $c$  and  $b$  quark events to determine the individual forward-backward asymmetries. In this analysis a simultaneous fit is performed in terms of the scaled energy  $X_E = 2E_D/\sqrt{s}$  and the  $b$ -tagging probability distribution. The forward-backward asymmetry is then extracted from the thrust polar angle distribution.

In this paper an update of previous DELPHI results [1] is presented. All LEP 1 data taken with the DELPHI detector in the years 1992 to 1995 are used. The high quality of the data through the final LEP 1 reprocessing in combination with improved reconstruction and  $b$ -tagging techniques [2] result in a significant gain in statistical precision.

## 2 The DELPHI Detector

A detailed description of the DELPHI detector can be found in [3]. Only the parts of the DELPHI detector which are important for this analysis will be briefly described in the following.

In the barrel region the innermost component is the vertex detector (VD) near to the LEP beam pipe. It consists of three concentric layers (closer,inner,outer) of silicon microstrip detectors. Since 1994 the VD provides in the closer and outer layer  $R\phi$  and  $z$  information and has an extended polar angle coverage of  $25^\circ < \theta < 155^\circ$  (closer layer).

The next component looking from the interaction point is the inner detector (ID). It consists of a jet-chamber to perform an precise  $R\phi$  measurement and five cylindrical MWPC layers. Since 1995 the MWPC are replaced by five layers of straw tube detectors.

The ID is followed by the TPC, the main tracking device in DELPHI. It covers polar angles between  $21^\circ < \theta < 159^\circ$  with a resolution of  $250 \mu\text{m}$  in  $R\phi$  and  $880 \mu\text{m}$  in  $z$ . The

---

<sup>1</sup>Throughout the paper charge-conjugated states are included implicitly.

analysis of the pulse height of the signals of the 192 signal wires allows the determination of the specific energy loss  $dE/dx$  which can be used for particle identification.

The barrel ring imagine Cherenkov counter (RICH) is placed behind the TPC. Its gas and liquid radiators allow particle identification over almost the whole momentum range.

The outer detector (OD) is mounted behind the RICH to give additional tracking information. It improves significantly the momentum resolution due to its large distance w.r.t. the interaction point. Five layers of drift cells cover polar angles between  $42^\circ < \theta < 138^\circ$  and provide  $R\phi$  and  $z$  information.

The barrel electromagnetic calorimeter (HPC) is placed between the OD and the superconducting coil and covers polar angles between  $42^\circ < \theta < 138^\circ$ . It is a gas-sampling device which provides complete three-dimensional charge information in the same way as a time projection chamber. The excellent granularity allows good separation between close particles in three dimensions. This permits good electron identification even inside jets and direct identification of  $\pi^0 \rightarrow \gamma\gamma$  decays.

In the forward region the tracking is performed by two planar drift chambers (FCA and FCB) with a polar angle covering of  $11^\circ < \theta < 33^\circ$  (FCA) and  $11^\circ < \theta < 36.5^\circ$  (FCB). Their resolutions in  $x$  and  $y$  are  $270 \mu m$  (FCA) and  $150 \mu m$  (FCB) respectively.

For muon identification the DELPHI detector is surrounded by layers of drift chambers. They cover  $52^\circ < \theta < 128^\circ$  with a resolution of  $4 mm$  in  $R\phi$  and  $2.5 cm$  in  $z$  in the barrel region and  $9^\circ < \theta < 43^\circ$  with a resolution of  $1 mm$  in the forward region.

### 3 Hadronic event selection

Before the track selection a primary vertex fit is performed. Using all charged tracks the primary vertex is fitted constrained by the beam spot position. Rejecting the tracks with the largest  $\chi^2$  contribution the fit is iterated until the  $\chi^2$  of each track is  $< 3$  or at least two tracks are left. For tracks measured in the forward region (FCA,FCB) the momentum resolution is improved by a track fit with primary vertex constraint. Forward tracks are removed if their  $\chi^2$  in the fit is  $> 100$ . After this procedure the following cuts are applied:

- momentum  $0.4 GeV < p < 50 GeV$  with  $\Delta p/p < 100 \%$
- track length  $L_{tr} > 30 cm$
- polar angle  $20^\circ < \theta < 160^\circ$
- closest impact to primary vertex  $\epsilon_{xy} < 4 cm$  and  $\epsilon_z < 10 cm$

The requirements for the event selection are:

- total charged energy  $\geq 12 \%\sqrt{s}$
- charged multiplicity  $\geq 5$

Only events taken on the  $Z$  pole are considered. A set of about 8.5 million hadronic Monte Carlo events for the years 1992 to 1995 are used. They are generated using Jetset 7.3 in combination with the full simulation of the DELPHI detector. The parameters of the generator are tuned to the DELPHI data [4]. Table 1 shows the number of selected hadronic events and the hadronic event efficiency. Remaining backgrounds from  $\tau$  pairs and Bhabha events are found to be negligible for this analysis.

Year	Data events	Monte Carlo events	efficiency
1992	703859	2003142	95.7 %
1993	475151	1893139	95.6 %
1994	1386191	3551362	95.7 %
1995	458700	1126557	95.8 %
92-95	3023901	8574200	95.7 %

Table 1: The number of selected hadronic events for data and Monte Carlo and the selection efficiency taken from the Monte Carlo.

## 4 Reconstruction of charmed mesons

Reconstructed  $D$  mesons are used as a signature for  $c\bar{c}$  and  $b\bar{b}$  events and are identified through their decay products. The  $D$  mesons are reconstructed in eight different decay modes. In the following a brief description of the selection criteria for the  $D$  candidates is given.

For all decay modes the selection of candidates is performed in a similar way. A number of charged particles with momentum  $p > 1 \text{ GeV}/c$  corresponding to the multiplicity of the specific  $D^{0/+}$  decay mode are combined, requiring the total charge to be zero in case of the  $D^0$  and one in case of  $D^+$  decays. The invariant mass  $m_D$  of the  $D^{0/+}$  candidate is calculated, assuming one of the particles to be a kaon and the others pions. In addition the kaon momentum has to exceed  $2 \text{ GeV}/c$ . A  $D^{*+}$  candidate is obtained by associating a low momentum pion to the reconstructed  $D^0$  meson. The charge of the pion is required to be opposite to that of the kaon from the  $D^0$  decay.

For the semileptonic decay modes  $D^0 \rightarrow K^- e^+ \nu$  and  $D^0 \rightarrow K^- \mu^+ \nu$  the lepton is required to be identified, using standard DELPHI identification criteria [3, 5]. For the reconstruction of  $\pi^0 \rightarrow \gamma\gamma$  decays,  $\pi^0$  with two photons merged in the HPC, two photons measured in the HPC or reconstructed from conversions are used [3, 6]. The particle identification provided by the RICH and the specific energy loss  $dE/dx$  measurement in the TPC were used to identify kaons. The tagging of the kaons was done using DELPHI standard tagging routines for the RICH [7] and the  $dE/dx$  [3] identification. For the RICH, the measured Cherenkov angle information was translated into  $\pi$ ,  $K$  and  $p$  tagging. The  $dE/dx$  information was only used if no RICH information was available. Here the tagging was done using the *pull* of the measured  $dE/dx$  w.r.t. the expected value for a given particle type.

For all decay modes a secondary vertex fit for the  $D^{0/+}$  is performed and the  $D^{0/+}$  flight distance and improved track parameters are obtained. All tracks associated to a  $D$  are required to have at least one hit in the vertex detector. A further reduction of background for the  $D^+$  is achieved by rejecting track combinations with a vertex  $\chi^2$  probability less than 0.001. The slow pion from the  $D^{*+}$  decay is constrained to the  $D^0$  vertex, which is a good approximation for the  $D^{*+}$  decay vertex because of the small transverse momentum of the slow pion with respect to the direction of flight of the  $D^0$ . Then the vertex information is used to improve the track parameters and thus the invariant mass resolution.



decay mode	$\Delta L$ for $D$ [cm]	$X_E^{cut}$	$x_{X_E}^{\Delta L}$	$y_{X_E}^{\Delta L}$	$x_{X_E}^{cos\Theta_H}$	$y_{X_E}^{cos\Theta_H}$
$D^{*+} \rightarrow (K^- \pi^+) \pi^+$	-0.05 to 2.0	0.15	-2.5	0.04	3.0	0.1
$D^{*+} \rightarrow (K^- \pi^+ \pi^- \pi^+) \pi^+$	0.0 to 2.0	0.3	-1.0	0.05	2.0	0.1
$D^{*+} \rightarrow (K^- \pi^+ \gamma \gamma) \pi^+$	0.0 to 2.0	0.3	-1.5	0.09	2.0	0.1
$D^{*+} \rightarrow (K^- \mu^+ \nu) \pi^+$	0.0 to 2.0	0.2	-1.2	0.06	3.0	0.1
$D^{*+} \rightarrow (K^- e^+ \nu) \pi^+$	0.0 to 2.0	0.2	-1.4	0.05	3.0	0.1
$D^{*+} \rightarrow (K^- \pi^+ (\pi^0)) \pi^+$	0.0 to 2.0	0.2	-2.5	0.03	3.0	0.0
$D^+ \rightarrow K^- \pi^+ \pi^+$	0.125 to 2.0	0.35	—	—	3.0	0.1
$D^0 \rightarrow K^- \pi^+$	0.05 to 2.0	0.3	-0.5	0.125	2.0	0.2
$D^0 \rightarrow K^- \pi^+ (\pi^0)$	0.05 to 2.0	0.3	-0.6	0.15	2.0	0.2

Table 2: Cuts for the  $X_E$  versus  $\Delta L$ .

The distance between the primary and the  $D^{0/+}$  vertex is calculated in the  $xy$  plane and projected onto the  $D^{0/+}$  direction of flight to obtain the decay length  $\Delta L$ . A vertex combination is accepted if  $\Delta L$  is within the range specified in table 2 for the different decay modes. In addition a cut is applied in the plane of  $X_E$  and  $\Delta L$  to reject combinatorial background, which is concentrated at low values of both of this variables.:

$$\Delta L(X_E) > x_{X_E}^{\Delta L} \cdot (X_E - X_E^{cut})^2 + y_{X_E}^{\Delta L} \quad (1)$$

The parameters are given in table 2.

Cuts on the helicity angle distribution (see table 2) are used to achieve a further significant reduction of the combinatorial background. The helicity angle  $\cos \theta_H$  is defined as the angle of the sphericity axis in the  $D^{0/+}$  rest frame with respect to the  $D^{0/+}$  direction of flight.  $D^{0/+}$  decays are isotropic in  $\cos \theta_H$ , whereas the background is extremely peaked at  $\cos \theta_H = \pm 1$ . Due to the energy spectrum of charged particles in hadronic  $Z$  events the combinatorial background is concentrated at small scaled energies  $X_E(D)$ . Therefore  $X_E$  dependent cuts on the helicity angle are used remove higher background contributions at small  $D$  energies.

$$X_E > 0.5 \cdot e^{\pm x_{X_E}^{cos\Theta_H} (\cos\Theta_H \mp 1)} - y_{X_E}^{cos\Theta_H} \quad (2)$$

In addition the  $X_E$  of the  $D$  combination is required to exceed the limits given in table 2, where also the parameters  $x_{X_E}^{cos\Theta_H}$  and  $y_{X_E}^{cos\Theta_H}$  are given.

The mass bands to select the different  $D^{0/+}$  decay modes and the cuts on the mass difference are listed in table 3. The mass differences and  $D^0$  and  $D^+$  mass distributions are shown in figures 1 and 2, respectively. The histograms show the simulated distributions normalized to the data samples. The contributions of signal and background are adjusted to compensate for different  $D$  rates in data and simulation.

For the  $D^+ \rightarrow K^- \pi^+ \pi^+$  mode a cut of  $\Delta m > 200$  MeV is used to veto  $D^{*+}$  decays. The wrong sign combination for  $D^0 \rightarrow K^- \pi^+$ , where the assignment of the kaon mass is used for the pion is also shown in the figure 2. An additional cut on the dalitz plot

mode	$D^{0/+}$ mass interval [GeV/ $c^2$ ]	max. $\Delta m$ [GeV/ $c^2$ ]
$D^{*+} \rightarrow (K^- \pi^+) \pi^+$	1.790 to 1.94	0.160
$D^{*+} \rightarrow (K^- \pi^+ \pi^- \pi^+) \pi^+$	1.845 to 1.90	0.160
$D^{*+} \rightarrow (K^- \pi^+ \gamma \gamma) \pi^+$	1.740 to 1.98	0.165
$D^{*+} \rightarrow (K^- \mu^+ \nu) \pi^+$	0.750 to 1.75	0.250
$D^{*+} \rightarrow (K^- e^+ \nu) \pi^+$	0.750 to 1.75	0.250
$D^{*+} \rightarrow (K^- \pi^+ (\pi^0)) \pi^+$	1.350 to 1.75	0.175
$D^+ \rightarrow K^- \pi^+ \pi^+$	1.700 to 2.05	-
$D^0 \rightarrow K^- \pi^+$	1.750 to 2.20	-
$D^0 \rightarrow K^- \pi^+ (\pi^0)$	1.500 to 1.70	-

Table 3: Cuts for the  $D$  selection.

for the  $D^{*+} \rightarrow (K^- \pi^+ \pi^0) \pi^+$  decay mode with a reconstructed  $\pi^0$  is applied to select the dominant decay via  $D^0 \rightarrow K^- \rho^+$ .

## 5 Measurement of $A_{FB}^c$ and $A_{FB}^b$

For a measurement of  $A_{FB}^c$  and  $A_{FB}^b$  from the polar angle  $\cos \theta_{thrust}$  of the thrust axis in the  $D$  meson events, it is necessary to separate  $D$  from  $c\bar{c}$  and  $b\bar{b}$  events and the combinatorial background. Since the  $c$  and  $b$  asymmetries are expected to be of comparable size and to have the same relative sign, the statistical precision of the measurement is limited by the negative correlation between both asymmetries. In this analysis, a good separation with a small correlation is obtained by using the scaled energy distribution  $X_E$  of the  $D$  candidates and the  $b$ -tagging probability  $\mathcal{P}_{ev}$ .

The hadronization of primary  $c$  quarks leads to high energy  $D$  mesons, whereas  $b$  quarks fragment into  $B$  hadrons which then decay into  $D$  mesons with a softer energy spectrum. On the other hand,  $b\bar{b}$  events can be identified due to the long lifetime of  $B$  hadrons, compared to the short lifetime of  $D$  mesons. Combinatorial background is concentrated at low  $X_E$  and is expected to have a flat distribution of the  $b$ -tag probability.

The shape of the combinatorial background is tested using the sidebands in the mass (or the mass difference) distribution. Due to the different relative acceptance of  $D$  mesons and background at small and large polar angles, the fit method has to account for the  $|\cos \theta_{thrust}|$  dependence of the different classes.

For the asymmetry measurement, partially reconstructed  $D^{*+}$  mesons ( $\pi_{sl} + X$ ) and reflections from other decay modes (see figures 1 and 2) have to be considered as signal to avoid charge correlations in the background. The contributions from reflections, where some particles from the  $D$  decay are assigned to wrong mass or are missing, and true  $D$  decays are treated as one class, because of the similar shape of the signals and the charge correlation with the primary quark. This leads to a significant increase of the sample for the  $K^- \pi^+ (\pi^0)$  decay mode. The rate of partially reconstructed  $D^{*+}$  mesons, where a slow pion from a  $D^{*+}$  decay is combined with a fake  $D^0$  candidate which includes some particles not from the  $D^0$  decay, depends on the branching ratio  $D^{*+} \rightarrow D^0 \pi^+$ , the  $D^{*+}$

production rate and the efficiency in the relevant mass difference interval. The contribution of partially reconstructed  $D^{*+}$  decays to the signal is taken from the simulation and contributes to the systematic error. In case of the  $D^0 \rightarrow K^- \pi^+ / K^- \pi^+ (\pi^0)$  decay modes without  $D^{*+}$  constraint the candidates with wrong mass assignments flip the sign of the estimated primary quark direction. This is taken into account in the fit.

To avoid double counting of events, only one  $D$  candidate in the signal region per event is retained. For a given event the  $D$  candidate with the largest kaon momentum is used. If two candidates use the same kaon track, the one with the largest  $X_E$  is used. Events entering the signal region for the  $K^- \pi^+$  decay mode are removed from the  $K^- \pi^+ \pi^- \pi^+$  distribution and events from both decay modes are then removed from the  $K^- \mu^+ \nu$  or  $K^- e^+ \nu$  distribution and so forth.

The number of reconstructed  $D$  decays given in table 4 is obtained from the fit to the mass spectra. A total sample of  $61829 \pm 521$  reconstructed  $D$  decays is used for the asymmetry measurement. The  $D$  mass bands to select  $D$  meson candidates are listed in table 3.

decay mode	signal events	signal region $\Delta m$ [GeV/ $c^2$ ]	signal region $m_D$ [GeV/ $c^2$ ]	$R_{S/B}$
$D^{*+} \rightarrow (K^- \pi^+) \pi^+$	$6030 \pm 103$	0.143-0.148	-	$0.95 \pm 0.02$
$D^{*+} \rightarrow (K^- \pi^+ \pi^- \pi^+) \pi^+$	$5123 \pm 103$	0.143-0.148	-	$0.86 \pm 0.02$
$D^{*+} \rightarrow (K^- \pi^+ \gamma \gamma) \pi^+$	$5787 \pm 125$	0.141-0.151	-	$1.19 \pm 0.03$
$D^{*+} \rightarrow (K^- \mu^+ \nu) \pi^+$	$3042 \pm 91$	$< 0.180$	-	$0.64 \pm 0.02$
$D^{*+} \rightarrow (K^- e^+ \nu) \pi^+$	$1810 \pm 65$	$< 0.180$	-	$0.98 \pm 0.04$
$D^{*+} \rightarrow (K^- \pi^+ (\pi^0)) \pi^+$	$15111 \pm 232$	$< 0.152$	-	$1.16 \pm 0.02$
$D^+ \rightarrow K^- \pi^+ \pi^+$	$5667 \pm 161$	-	1.83-1.91	$0.83 \pm 0.02$
$D^0 \rightarrow K^- \pi^+$	$9311 \pm 232$	-	1.80-1.93	$1.00 \pm 0.02$
$D^0 \rightarrow K^- \pi^+ (\pi^0)$	$9948 \pm 298$	-	1.50-1.70	$1.21 \pm 0.04$

Table 4:  $D$  mesons sample used for the measurement, cuts to select signal region and the relative normalization  $R_{S/B}$  of signal to background.

## 5.1 The minimum $\chi^2$ fit

The determination of the asymmetries is achieved by a minimum  $\chi^2$  fit to the  $D$  samples using the scaled energy ( $X_E$ ), the  $b$ -tagging probability ( $tr(\mathcal{P}_{ev})$ ) and the polar angle ( $\cos \theta_{thrust}$ ). An example for these distributions for the  $D^{*+} \rightarrow (K^- \pi^+) \pi^+$  channel are shown in figure 3. The measured distributions are compared to the predictions of the simulation, split into charm, bottom and background events. The simulated prediction is normalized to the data to reproduce the signal to background ratio. Therefore a factor  $R_{S/B}$  (see table 4) is introduced for each decay mode, which compensates for different  $D$  rates in data and simulation. After this correction a good agreement is found in all distributions. The shape of the background distribution, as obtained from the sidebands, is well reproduced by the Monte Carlo.

For the  $b$ -tagging probability distribution a transformation:

Decay mode	number of bins per			average number of events
	$X_E$	$tr(\mathcal{P}_{ev})$	$\cos \theta_{thrust}$	
$D^{*+} \rightarrow (K^- \pi^+) \pi^+$	4	5	4	77.9
$D^{*+} \rightarrow (K^- \pi^+ \pi^- \pi^+) \pi^+$	5	5	5	65.8
$D^{*+} \rightarrow (K^- \pi^+ \gamma \gamma) \pi^+$	4	4	4	88.0
$D^{*+} \rightarrow (K^- \mu^+ \nu) \pi^+$	4	6	4	49.5
$D^{*+} \rightarrow (K^- e^+ \nu) \pi^+$	4	4	3	56.3
$D^{*+} \rightarrow (K^- \pi^+ (\pi^0)) \pi^+$	6	7	5	77.7
$D^+ \rightarrow K^- \pi^+ \pi^+$	5	5	5	87.9
$D^0 \rightarrow K^- \pi^+$	5	6	5	80.0
$D^0 \rightarrow K^- \pi^+ (\pi^0)$	7	7	7	59.9

Table 5: Number of bins in each dimension used for the individual decay modes and the average number of data events per bin.

$$tr(\mathcal{P}_{ev}) = \frac{2.5}{5.1 - \mathcal{P}_{ev}} \quad (3)$$

was used. Bins in the three dimensional  $X_E$ ,  $tr(\mathcal{P}_{ev})$  and  $\cos \theta_{thrust}$  space have been chosen such that each bin contains about 70 events (table 5). In each bin  $i$  the differential asymmetry:

$$A_{FB}^{obs,i} = \frac{N_i^+ - N_i^-}{N_i^+ + N_i^-} \quad (4)$$

is calculated from the events  $N_i^+$  and  $N_i^-$  with  $Q \cdot \cos \theta_{thrust}$  greater or less than zero, respectively. The observed asymmetry receives contributions from  $c$ ,  $b$  and combinatorial background. The fractions  $f_{j,i}$  of  $D$  signal and reflection from  $c$  and  $b$  events as well as the fractions of partially reconstructed  $D$  mesons and combinatorial background are taken from the simulation. Furthermore the combinatorial background is divided into  $c$ ,  $b$  and  $uds$  contributions to account for small charge correlation in the background especially for the semileptonic decay mode of the  $D^0$

The  $\chi^2$  to be minimized is given by:

$$\chi^2 = \sum_{i=1}^{N_{bins}} \left\{ A_{FB}^{obs,i} - \sum_{j=1}^7 f_{j,i} C_{j,i} A_{FB}^j(\cos \theta) \right\}^2 / \sigma_i^2 \quad (5)$$

where  $\sigma_i$  allows for the statistical error of both, data and simulation.  $A_{FB}^j(\cos \theta)$  is the differential asymmetry:

$$A_{FB}^j(\cos \theta) = \frac{8}{3} A_{FB}^j \frac{\cos \theta}{1 + \cos^2 \theta}, \quad (6)$$

of  $b$ ,  $c$  or  $uds$  events. In each bin the average polar angle  $\cos \theta_f$  of the primary quarks after photon radiation from the simulation was used. That way the QCD corrections [9] are taken into account in the fit.  $C_{j,i}$  is the charge correlation of the class  $j$  calculated in

each bin using the simulation. For  $b$  events the mixing effect as a function of the  $b$ -tagging probability has to be taken into account leading to smaller values of  $C_{j,i}$  and thus to a smaller observed  $b$  asymmetry. See section 6 for details. The combinatorial background from  $c$  is expected to have only small charge correlation  $C_{j,i}$  to the primary quark at large energies  $X_E$ . The asymmetry of the combinatorial background and  $D$  mesons from gluon splitting in  $uds$  events is expected to be very small. The predictions from the simulations for each bin are subtracted in the fit. The agreement of data and simulation was tested in the sidebands of the different samples where no deviations have been found.

## 6 Effective mixing in $b \rightarrow D$ decays

The observed forward-backward asymmetry in  $b$  events is proportional to the charge correlation of the reconstructed  $D$  meson to the primary quark. The correlation  $C_b$  is reduced due to the  $B^0 - \bar{B}^0$  mixing by a factor  $1 - 2\chi$ . The mixing probability  $\chi$  determined by the mass difference  $\Delta m$  between the two mass eigenstates and the  $B$  lifetime  $\tau_B$ . The product of both is measured to be  $\chi_d = 0.172 \pm 0.010$  [8]. For the  $B_s^0$  only an upper limit of  $\Delta m_s > 14 \text{ ps}^{-1}$  [8] is known. This is compatible with full mixing  $\chi_s \sim 0.5$ .

The production of  $D$  mesons from the upper vertex (the  $W$  decay) also reduces the charge correlation to the primary  $b$  quark. A sizeable rate  $f_{B \rightarrow W \rightarrow D}$  of wrong sign  $D$  mesons from  $B$  decays reduces the measured  $b$  asymmetry by a factor  $1 - 2f_{B \rightarrow W \rightarrow D}$ . Recent measurements of CLEO and ALEPH indicate a significant rate of double-charmed  $B$  decays involving no  $D_s$  production. CLEO [10] finds for the sum of  $B_d^0$  and  $B^+$  a ratio of:

$$\frac{\Gamma(B \rightarrow DX)}{\Gamma(B \rightarrow \bar{D}X)} = 0.100 \pm 0.026 \pm 0.016. \quad (7)$$

This number is in good agreement with the result from ALEPH [11]:

$$BR(b \rightarrow D^0 \bar{D}^0, D^0 D^-, D^+ \bar{D}^0 + X) = 7.8_{-1.8}^{+2.0} {}_{-1.5}^{+1.7} {}_{-0.4}^{+0.5} \%, \quad (8)$$

where the dominant contribution is  $B \rightarrow D^{(*)} \bar{D}^{(*)} K$ . Both measurements include cabbibo suppressed  $W \rightarrow c\bar{d}$  decays which are expected to contribute about 1 % to the upper vertex charm rate.

The observed  $b$  forward-backward asymmetry in the different  $D$  samples needs to be corrected for both effects. The visible size of both effects depends on details in the  $B \rightarrow D$  decay properties, because the mixing is visible in  $D$  mesons from  $B_d^0$  and  $B_s^0$  decays, but not in  $B^+$  or  $\Lambda_b$  decays. The fractions of  $D^+$ ,  $D^0$  and  $D^{*+}$  from different  $B$  states need to be determined from the branching rates  $B \rightarrow D$ . Very little is known at present about the individual exclusive branching ratios  $B \rightarrow D + X$ , but several inclusive measurements from the  $\Upsilon 4S$  and LEP experiments can be used to deduce the rates.

CLEO and ARGUS have measured the rates [8] of  $D^0$ ,  $D^+$ ,  $D_s^+$  and  $\Lambda_c$  as well as the rates of  $D^{*+}$  and  $D^{*0}$  in  $\Upsilon 4S$  decays, i.e. in decays of  $B_d^0$  and  $B^+$  at 50 % admixture. From these measurements the overall rates of  $B_d^0$  and  $B^+$  decays in the  $D$  samples are deduced taking into account the production fractions of  $B^+$ ,  $B_d^0$ ,  $B_s^0$  and  $\Lambda_b$  in  $Z \rightarrow b\bar{b}$  events [8]. The rate of  $D^{*+}$  from  $B^+$  and  $B^0$  is not measured. Therefore the JETSET prediction of  $B^+ \rightarrow D^{*\pm} + X / B^{+,0} \rightarrow D^{*\pm} + X = 0.30$  with an relative error of 50 % was

used. This number is compatible with the assumption that most of the  $B^+ \rightarrow D^{*\pm} + X$  decays via higher  $D$  resonances.

The vector rates measured at the  $\Upsilon 4S$  also fix the effective rate of vector and pseudo scalar mesons  $V/(V + P)$ . The decay of the  $D^{*0}$  into  $D^+\pi^-$  is forbidden by phase space, while the branching ratio  $D^{*+} \rightarrow D^0\pi^+$  is measured to  $0.683 \pm 0.013$  [8]. This difference in  $D^{*+}$  and  $D^{*0}$  decays affects significantly the fraction of  $B^+$  and  $B_d^0$  decays seen in the  $D^{(*)+}$  and  $D^0$  samples and thus the effective mixing.

A small correction to the  $B^+$  and  $B_d^0$  into  $D^+$ ,  $D^0$  and  $D^{*+}$  rates originates from  $D^{**}$  production. These states subsequently decay into vector or pseudo scalar states.  $D_2^*$  mesons decay into  $D^*$  and  $D$  states, while angular momentum conservation allows  $D^0$  mesons to decay into  $D$  states and  $D_1$  and  $D^{*0}$  decay into  $D^*$  mesons. The decay rates of the different  $D^{**}$  states into vector and pseudo scalar states are fixed by isospin invariance and the measured ratio  $BR(D_2^{*0} \rightarrow D^+\pi^-)/BR(D_2^{*0} \rightarrow D^{*+}\pi^-) = 2.3 \pm 0.8$  [12]. The relative production rates of the four  $D^{**}$  states are assumed to be proportional to the number of spin states. The total  $D^{**}$  rate is obtained from the measured semileptonic  $B$  branching ratios  $BR(B \rightarrow D^{**l^+\nu})/BR(B \rightarrow Xl^+\nu) = 0.26 \pm 0.07$  [8].

The decay of  $B_s^0$  and  $\Lambda_b$  into  $D^+$ ,  $D^0$  and  $D^{*+}$  also contributes to the sample. They can be deduced from the total rate of  $D^0$ ,  $D^+$ ,  $D_s^+$  and  $\Lambda_c$  in  $Z \rightarrow b\bar{b}$  events measured at LEP [13]. Here the number of charm quarks produced per  $b$  decay is limited to the LEP measurement  $n_c = 1.17 \pm 0.04$  [8] taking charmonia and  $\Xi_c$  production into account.

From this information and assuming that  $W \rightarrow c\bar{s} \rightarrow D^{(*)+}$  is equal to  $W \rightarrow c\bar{s} \rightarrow D^{(*)0}$  one obtains for the effective mixing seen in the  $D^+$ ,  $D^0$  and  $D^{*+}$  samples:

$$\chi_{eff}(D^+) = 0.222 \pm 0.033 \quad (9)$$

$$\chi_{eff}(D^0) = 0.176 \pm 0.030 \quad (10)$$

$$\chi_{eff}(D^{*+}) = 0.222 \pm 0.033 \quad (11)$$

The errors quoted represent the precision of the measurements used to determine the  $b$  decay properties. The effective mixing for the  $D^{*+}$  sample is in good agreement with a direct measurement of OPAL using the jet charge technique in the opposite hemisphere w.r.t. the reconstructed meson. They obtained  $\chi_{eff}(D^{*+}) = 0.191 \pm 0.083$  [15].

## 7 Systematic uncertainties

The systematic error sources are of two types. The uncertainty of the Monte Carlo modelling of heavy quark production affect the measurement. Also problems in the simulation description of the background as well as the fit method itself are potential sources of systematic errors.

It is necessary to correct for inadequate simulation settings to correctly describe the heavy quark production. The corrections are done using JETSET to produce the required distribution and compare it to the one given in the full simulation before detector acceptance. The ratio of the two spectra is used as a weight to modify the Monte Carlo shape in equation 5. To estimate the systematic error the input value is changed within its error and the procedure is repeated.

To allow for the uncertainty of the mean  $\langle X_E^c(D) \rangle$  and  $\langle X_E^b(B) \rangle$  the procedure is quite similar. JETSET is used to generate the  $\langle X_E \rangle$  distributions of all charm ground states

systematic error source	variation	$\delta A_{\text{FB}}^c$	$\delta A_{\text{FB}}^b$
MC statistics	see text	$\pm 0.00235$	$\pm 0.00336$
$\langle X_E \rangle_{D^*}$	$0.510 \pm 0.009$	$\pm 0.00035$	$\mp 0.00098$
$\langle X_E \rangle_B$	$0.702 \pm 0.008$	$\mp 0.00023$	$\pm 0.00015$
$\epsilon_{B \rightarrow D}$	$0.42 \pm 0.07$	$\pm 0.00028$	$\mp 0.00037$
$\tau_b(B^+, B^0, B_s^0, \Lambda_b)$	see text	$\mp 0.00015$	$\mp 0.00016$
$\tau_c(D^+, D^0, D_s^+, \Lambda_c)$	see text	$\pm 0.00005$	$\pm 0.00005$
$f(D^+), f(D_s^+), f(\Lambda_c)$	see text	$\pm 0.00022$	$\mp 0.00029$
$n_{g \rightarrow c\bar{c}}$	$2.38 \pm 0.48 \%$	$\pm 0.00002$	$\pm 0.00025$
$(R_b \cdot P_{b \rightarrow D}) / (R_c \cdot P_{c \rightarrow D})$	see text	$\pm 0.00037$	$\mp 0.00026$
$B^0 - \bar{B}^0$ mixing	see text	$\mp 0.00011$	$\pm 0.00595$
QCD bias	see text	$\mp 0.00026$	$\mp 0.00053$
fit method	see text	$\pm 0.00168$	$\pm 0.00253$
$R_{S/B}$	$\pm 5\%$	$\mp 0.00069$	$\mp 0.00126$
$\pi_{\text{slow, wrong sign}}$	$\pm 30\%$	$\mp 0.00025$	$\pm 0.00246$
$A_{\text{FB}}^{uds}(\text{background})$	$\pm 100\%$	$\pm 0.00171$	$\mp 0.00018$
$A_{\text{FB}}^{b,c}(\text{background})$	$\pm 50\%$	$\mp 0.00237$	$\mp 0.00597$
total	—	$\pm 0.00424$	$\pm 0.00990$

Table 6: Contributions to the systematic errors on the measured asymmetries.

according to  $\langle X_E^c(D^*) \rangle = 0.510 \pm 0.005 \pm 0.008$ ,  $\langle X_E^b(B) \rangle = 0.702 \pm 0.008$  [16]. The energy spectrum of  $D$  mesons in the  $B$  rest frame was measured by CLEO [17]. This  $\langle X_E^b(D) \rangle$  spectrum includes the contributions from  $B \rightarrow D X$  and  $B \rightarrow D \bar{D} X$ . It can be parameterised in terms of a Peterson function with  $\epsilon_{b \rightarrow D} = 0.42 \pm 0.07$  [18].

The corrections are applied on all simulated charm ground state hadrons separately for  $b\bar{b}$  and  $c\bar{c}$  events. The resulting  $X_E$  distribution of the sum of all charm hadron ground states in  $c\bar{c}$  events is found to be in agreement with the corresponding average of  $\langle X_E^c(D^0, D^+) \rangle = 0.484 \pm 0.008$  [16]. Here the effect of gluon splitting is taken into account. The systematic uncertainties are calculated separately for  $\langle X_E^c(D) \rangle$ ,  $\langle X_E^b(B) \rangle$  and  $\epsilon_{b \rightarrow D}$ .

The  $b$  lifetimes are corrected separately for  $B^+$ ,  $B^0$ ,  $\Lambda_b$  and  $B_s^0$ . Here the world averages  $\tau(B^0) = 1.56 \pm 0.04$ ,  $\tau(B^+) = 1.65 \pm 0.04$ ,  $\tau(B_s^0) = 1.54 \pm 0.07$  and  $\tau(\Lambda_b) = 1.22 \pm 0.05$  [8] are used to correct the simulation. For the systematic uncertainties belonging to this source all the  $b$  lifetime distributions are regenerated with 1 sigma variation and the fit is performed again. Similar to this procedure the  $c$  lifetimes are also corrected separately for  $D^+$ ,  $D^0$ ,  $\Lambda_c$  and  $D_s^+$ . Here the values  $\tau(D^0) = 0.415 \pm 0.004$ ,  $\tau(D^+) = 1.057 \pm 0.015$ ,  $\tau(D_s^+) = 0.467 \pm 0.017$  and  $\tau(\Lambda_c) = 0.206 \pm 0.012$  from [16] are taken.

The separation between  $b\bar{b}$  and  $c\bar{c}$  events obtained from the impact parameter tag depends on the rate of  $D^+$  and  $D^0$  mesons in  $c\bar{c}$  events. Therefore the rates of charm hadrons in the hemisphere opposite to the reconstructed  $D$  are fixed to the present averages  $f(D^+) = 0.221 \pm 0.020$ ,  $f(D_s^+) = 0.112 \pm 0.027$  and  $f(c_{\text{baryon}}) = 0.084 \pm 0.022$  [19]. The  $D^0$  rate is calculated from these numbers according to:

$$f(D^0) = 1 - f(D^+) - f(D_s^+) - f(c_{baryon}). \quad (12)$$

A variation of one standard deviation on each fraction is included in the systematic error, leaving the  $D^0$  fraction free to keep the sum constant.

The rate of gluon splittings into  $c\bar{c}$  pairs was varied within one standard deviation. The relative rate of  $D$  mesons from  $b\bar{b}$  and  $c\bar{c}$  events is not a free parameter in the asymmetry fit. Therefore the ratio was fixed to the DELPHI measurement [14] using the same data and varied within 1 sigma.

The mixing correction for the  $A_{FB}^b$  was discussed in section 6. The systematic error is obtained by varying separately each parameter used to obtain the  $B$  decay rates into  $D$  mesons by 1 sigma. The effect of the variation was studied directly on the asymmetry fit to allow for the lifetime dependence of the  $B^0 - \bar{B}^0$  mixing. The total error is then calculated taking the correlation between the parameters into account. The oscillation frequency error is small compared to the uncertainty of the  $B \rightarrow D$  rates.

The asymmetry fit was done using the quark axis in the simulation. Therefore most of the QCD corrections[9] are implicitly taken into account. The experimental bias was studied using a fit to the simulation after setting the generated asymmetry to 75%. The observed relative difference of  $+0.5 \pm 0.06\%$  for  $c\bar{c}$  and  $+1.7 \pm 0.08\%$  for  $b\bar{b}$  events is used to define the experimental bias on the QCD corrections which was used to correct the fit results. The statistical error of the fit and the uncertainty of the QCD correction are used to determine the systematic error.

Differences between the signal and background efficiency as a function of  $\cos\theta$  are considered in the calculation of the probabilities from the simulation. Since the asymmetry enters in the  $\chi^2$  as a function of  $\cos\theta$ , the sensitivity to efficiency variations is small. The systematic error due to the fit method is estimated by comparing the results of the  $\chi^2$  fit to the results obtained assuming a Poissonian distribution and neglecting in both cases the error on the simulation. The observed difference is included in the systematic error.

For all decay modes the relative normalization  $R_{S/B}$  is obtained from a fit of the simulated  $D$  signal and background to the data. A variation of  $\pm 5\%$  is included in the systematic error, not only to account for the error of the fitted  $R_{S/B}$ , but also for uncertainties in the agreement of the shape of the mass difference signals in data and simulation.

The systematic error due to the contribution of partially reconstructed  $D$  decays is estimated by a 30% variation of the prediction of the simulation. This includes uncertainties on the efficiency to reconstruct such  $\pi_{sl} + X$  combinations as well as on the total rate of  $D^{*+} \rightarrow D^0\pi^+$  decays in hadronic  $Z$  events.

The asymmetry of the  $uds$  quark background is taken from the simulation and subtracted in the fit. The agreement between data and simulation is tested using the side bands, where good agreement is found. A 100% variation enters into the systematic error. The charge correlation for the combinatorial background from  $b$  and  $c$  events is taken from the simulation. A variation of 50% has been considered in the systematic error on the asymmetry.

The contributions to the systematic errors for the combined fit of the charm and bottom asymmetries are listed in table 6. The relative sign of the systematic error indicates the direction in which the results change for a particular error source.



## 8 Fit results

decay mode	$A_{FB}^{c\bar{c}}$		$A_{FB}^{b\bar{b}}$		correlation	$\chi^2/N.D.F.$
$D^{*+} \rightarrow (K^- \pi^+) \pi^+$	0.0577	$\pm$ 0.0237	0.0498	$\pm$ 0.0476	-0.26	1.02
$D^{*+} \rightarrow (K^- \pi^+ \pi^- \pi^+) \pi^+$	0.0758	$\pm$ 0.0235	0.1139	$\pm$ 0.0546	-0.28	0.86
$D^{*+} \rightarrow (K^- \pi^+ \gamma \gamma) \pi^+$	0.0261	$\pm$ 0.0298	0.0881	$\pm$ 0.0634	-0.28	0.79
$D^{*+} \rightarrow (K^- \mu^+ \nu) \pi^+$	0.1133	$\pm$ 0.0321	0.0141	$\pm$ 0.0723	-0.25	1.11
$D^{*+} \rightarrow (K^- e^+ \nu) \pi^+$	0.1236	$\pm$ 0.0434	0.0167	$\pm$ 0.0997	-0.22	1.27
$D^{*+} \rightarrow (K^- \pi^+ (\pi^0)) \pi^+$	0.0712	$\pm$ 0.0207	0.1084	$\pm$ 0.0459	-0.27	0.93
$D^+ \rightarrow K^- \pi^+ \pi^+$	0.0563	$\pm$ 0.0251	0.0072	$\pm$ 0.1234	-0.33	1.01
$D^0 \rightarrow K^- \pi^+$	0.0452	$\pm$ 0.0370	0.0748	$\pm$ 0.0480	-0.37	0.76
$D^0 \rightarrow K^- \pi^+ (\pi^0)$	0.0430	$\pm$ 0.0402	0.0989	$\pm$ 0.0480	-0.34	0.80
Average	0.0658	$\pm$ 0.0093	0.0766	$\pm$ 0.0190	-0.27	0.61

Table 7: Fit results of the two parameter fit to the individual decay modes. The average centre of mass energy is 91.235 GeV.

The results of the 2 parameter fits of the  $c$  and  $b$  asymmetries is given in table 7. Combining the results of the different samples leads to:

$$A_{FB}^c = 0.0658 \pm 0.0093(stat) \quad (13)$$

$$A_{FB}^b = 0.0766 \pm 0.0190(stat) \quad (14)$$

with a statistical correlation of  $-0.27$ . The average centre of mass energy is  $\sqrt{s} = 91.235$  GeV. In figure 4 the fit results for the forward-backward asymmetries of the different samples are compared to the average. The forward-backward asymmetry averaged over all samples as a function of  $\cos \theta_{thrust}$  is shown in figure 5.

## 9 Conclusion

A measurement of the  $A_{FB}^c$  and  $A_{FB}^b$  on the  $Z$  resonance is performed using about 3 million hadronic  $Z$  decays collected by the DELPHI detector at LEP in the years 1992 to 1995. The heavy quark is tagged by the exclusive reconstruction of  $D$  meson decays in the modes  $D^{*+} \rightarrow D^0 \pi^+$ ,  $D^0 \rightarrow K^- \pi^+$  and  $D^+ \rightarrow K^- \pi^+ \pi^+$ . The forward-backward asymmetries for  $c$  and  $b$  quarks at the  $Z$  resonance are determined to be:

$$A_{FB}^c = 0.0658 \pm 0.0093(stat) \pm 0.0042(syst) \quad (15)$$

$$A_{FB}^b = 0.0766 \pm 0.0190(stat) \pm 0.0099(syst) \quad (16)$$

with a total correlation of  $-0.16$ . The results are in good agreement with other LEP measurements [19].

## 10 Acknowledgements

We thank the SL division of CERN for the excellent performance of the LEP collider and their careful work on the beam energy determination. We are also grateful to the technical and engineering staffs in our laboratories and to our funding agencies for their continuing support.

## References

- [1] P.Abreu et al., DELPHI Collaboration, *Measurement of the forward - backward asymmetry of charm and bottom quarks at the Z pole using  $D^{*+-}$  mesons*, Z. Phys. **C66** (1995) 341-354
- [2] G.J.Barker et al., DELPHI Collaboration, *A precise measurement of partial decay width ratio  $R_b^0 = \Gamma_{b\bar{b}}/\Gamma_{had}$* , ICHEP'98 #123, DELPHI 98-123 CONF 184, Geneva 1998
- [3] P.Abreu et al., DELPHI Collaboration, Nucl. Inst. and Meth. **A 378** (1996) 57
- [4] P.Abreu et al., DELPHI Collaboration, *Tuning and test of fragmentation models based on identified particles and precision event shape data*, Z. Phys. **C73** (1996) 11-60
- [5] C.Kreuter, *Electron Identification using a Neural Network*, DELPHI 96-196 PHYS 658, Geneva 1996
- [6] C.Kreuter, M.Feindt, O.Podobrin, *ELEPHANT Reference Manual*, DELPHI 96-82 PROG 217, Geneva 1996
- [7] E.Schyns, *NEWTAG -  $\pi$ , K, p Tagging for DELPHI RICHes*, DELPHI 96-103 RICH 89, Geneva 1996
- [8] Review of Particle Physics, Euro. Phys. J. **C3** (1998) 1
- [9] D.Abbaneo et al., *QCD corrections to the forward-backward asymmetries of c and b quarks at the Z pole*, CERN-EP/98-32, Geneva 1998, submitted to Eur.Phys.J.C.
- [10] T.E.Coan et al., CLEO Collaboration, *Flavour-Specific Inclusive B Decays to Charm*, CLNS 97/1516, CLEO 97-23
- [11] R.Barate et al., ALEPH Collaboration, *Observation of doubly-charmed B decays at LEP*, CERN-EP/98-037, Geneva 1998
- [12] H.Albrecht et al., ARGUS Collaboration, Phys. Lett. **B 232** (1989) 398,  
P.Avery et al., CLEO Collaboration, Phys. Lett. **B 331** (1994) 236
- [13] D.Buskulic et al., ALEPH Collaboration, Phys. Lett. **B 388** (1996) 648,  
G.Alexander et al., OPAL Collaboration. Z. Phys. **C 72** (1996) 1

- [14] D.Bloch et al., DELPHI Collaboration, *Measurement of the Z Partial Decay Width into  $c\bar{c}$  and Multiplicity of Charm Quarks per b Decay*, ICHEP'98 #122, DELPHI 98-120 CONF 181, Geneva 1998
- [15] G.Alexander et al., OPAL Collaboration, *Z. Phys. C* **73** (1997) 379
- [16] The LEP Electroweak Working Group, *Presentation of LEP Electroweak Heavy Flavour Results for the Summer 1996 Conferences*, LEPHF/96-01, DELPHI 96-67 PHYS 627, Geneva 1996
- [17] D.Bortoletto et al., CLEO Collaboration, *Phys. Rev. D* **45** (1992) 21
- [18] The LEP Electroweak Working Group, *A consistent treatment of systematic Errors for LEP electroweak Heavy Flavour Analyses*, LEPHF/94-01, DELPHI 94-23 PHYS 357
- [19] The LEP Electroweak Working Group, *A Combination of Preliminary Electroweak Measurements and Constraints on the Standard Model*, CERN-PPE/97-154, Geneva 1997

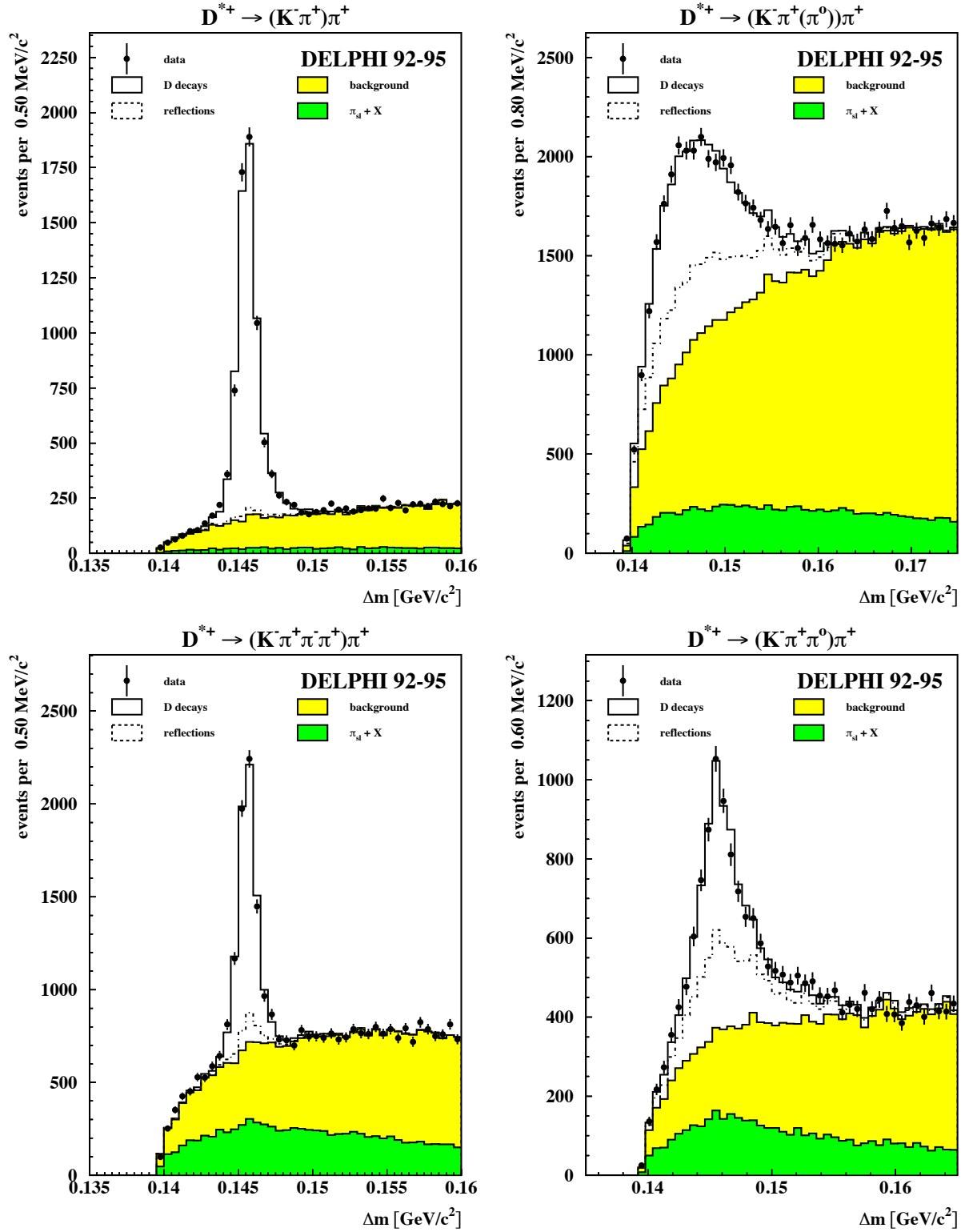


Figure 1: The mass difference distributions  $\Delta m$  for the different decay modes.  $\Delta m$  is defined as the difference between the mass of the  $D^{*+}$  and the  $D^0$  candidate. The data are compared to the simulation. Contributions from reflections, partially reconstructed  $D^{*+}$  decays ( $\pi_{sl} + X$ ) and combinatorial background are also shown. See section 5 for the discussion of these contributions

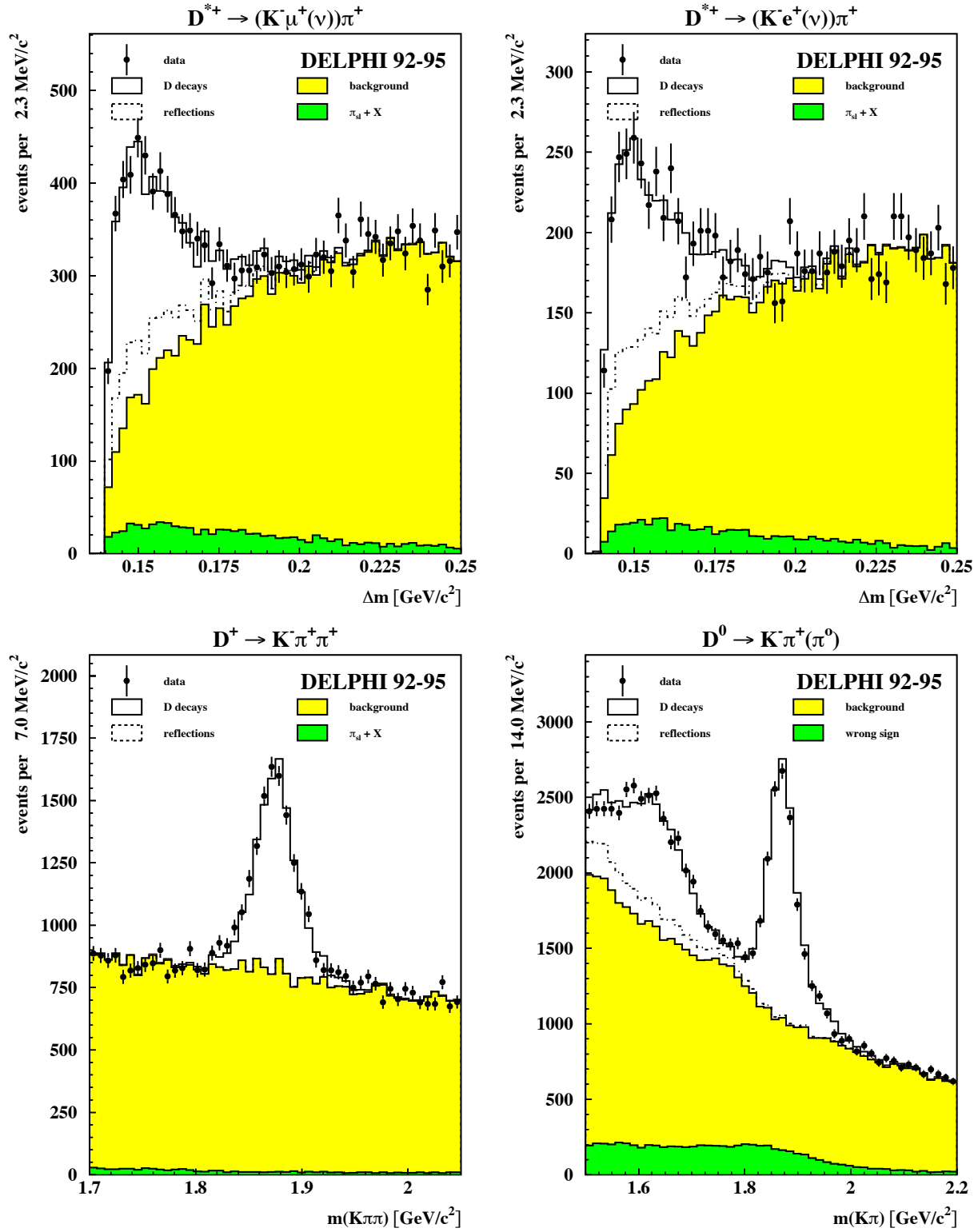


Figure 2: The mass difference distributions  $\Delta m$  for the semileptonic decay modes are shown above.  $\Delta m$  is defined as the difference between the mass of the  $D^{*+}$  and the  $D^0$  candidate. The data are compared to the simulation. Contributions from reflections, partially reconstructed  $D^{*+}$  decays and combinatorial background are also shown. The picture below shows the  $D^0$  and  $D^+$  mass distributions. For the  $D^0$  the background composition of candidates with wrong mass assignment is also shown.

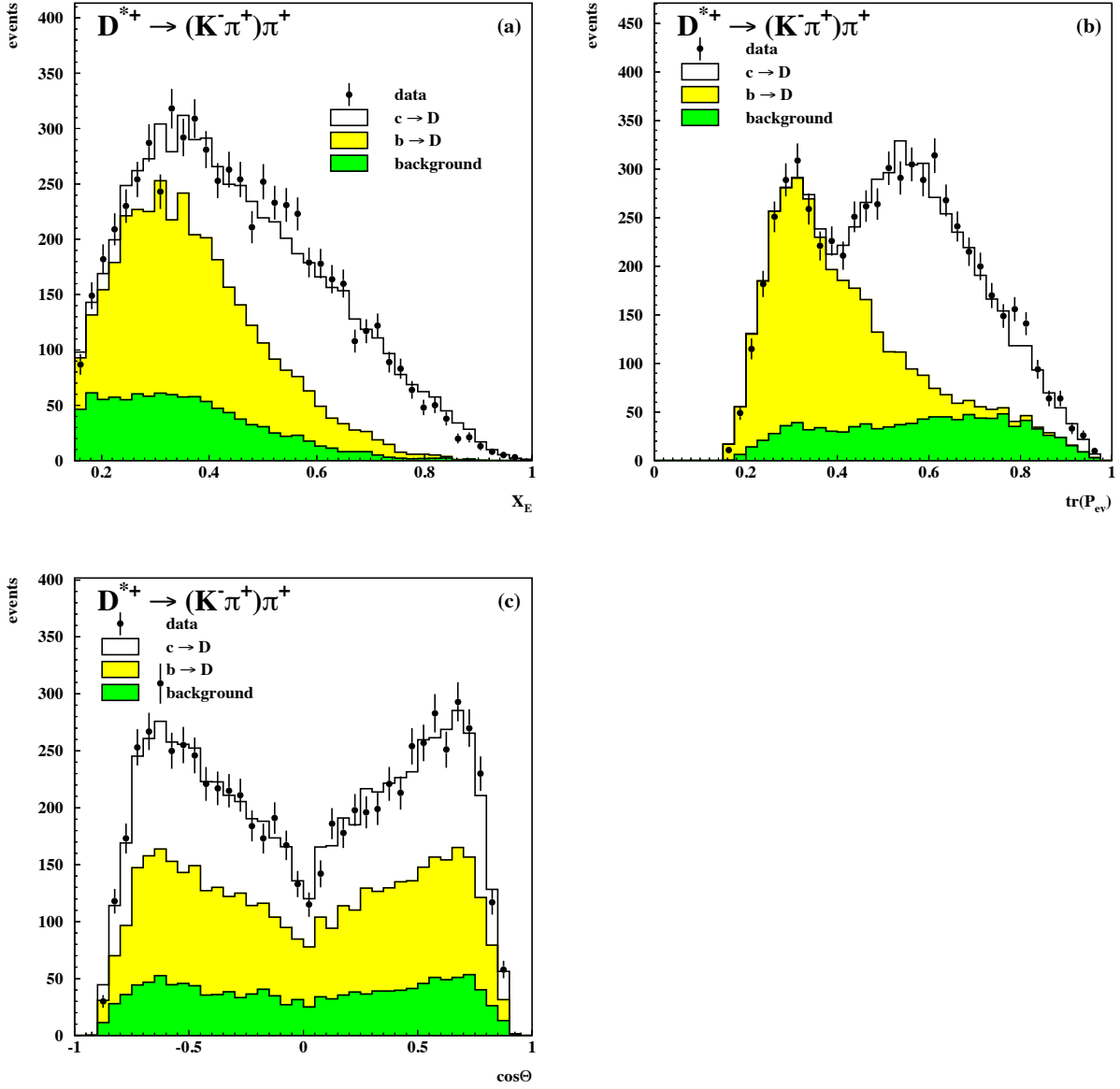


Figure 3: The  $X_E$ ,  $tr(\mathcal{P}_{ev})$  and  $\cos(\theta)$  distribution for the signal region of the  $D^{*+} \rightarrow (K^- \pi^+) \pi^+$  decay mode. The data are compared to simulation where  $D^{*+}$  from charm and bottom events and combinatorial background are shown separately. See section 5.1 for the definition of the transformation  $tr(\mathcal{P}_{ev})$ .

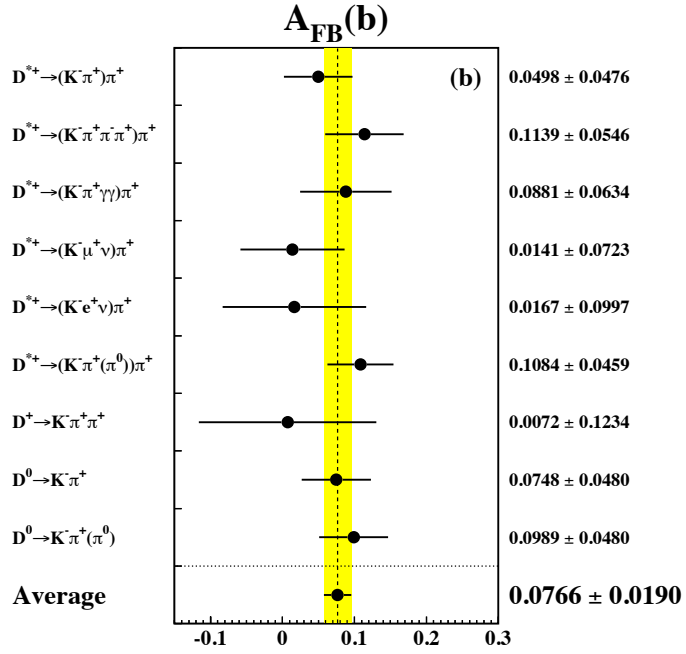
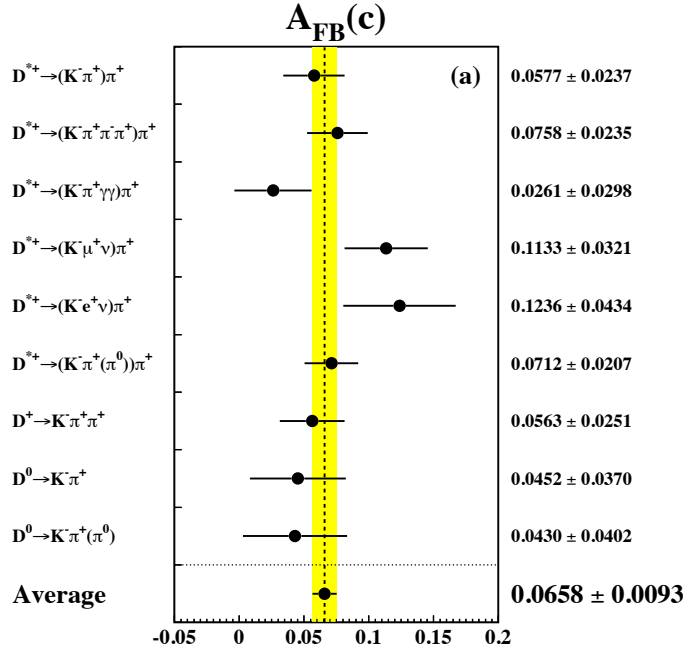


Figure 4: The results of the two parameter fit of the  $c$  and  $b$  asymmetry at an average centre of mass energy of 91.235 GeV for the different  $D$  samples are shown. The grey band represents the average over all these measurements. Only statistical errors are shown.

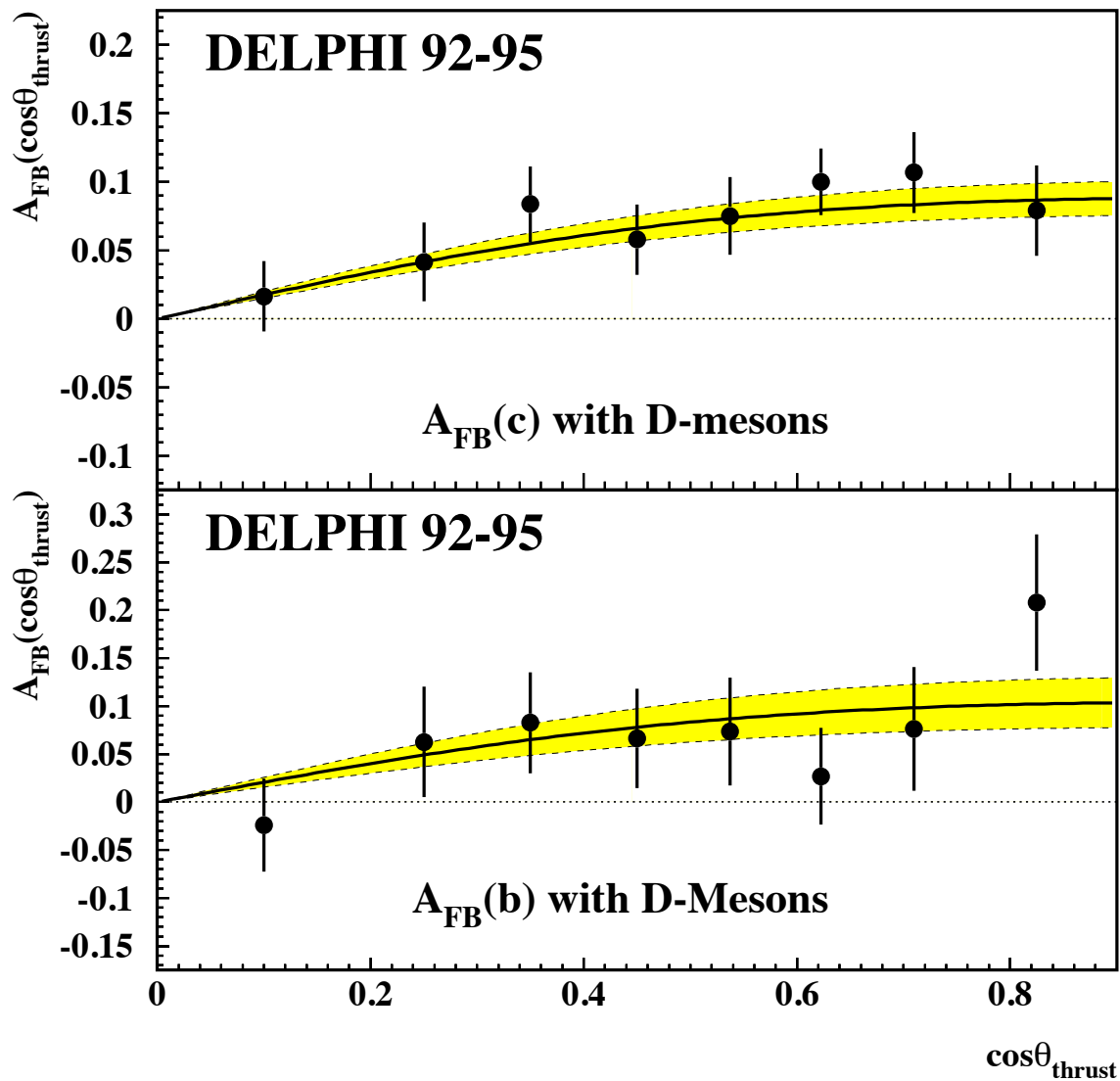


Figure 5: The  $c$  and  $b$  forward-backward asymmetries at an average centre of mass energy of 91.235 GeV as a function of  $\cos\theta$ . Only statistical errors are shown. The bands represent the fit results.